Turbulence characteristics in a free wake of an actuator disk: comparisons between a rotating and a non-rotating actuator disk in uniform inflow

H Olivares-Espinosa[1], S-P Breton[2], C Masson[1] and L Dufresne[1]

[1] Département de génie mécanique, École de technologie supérieure, 1100, rue Notre-Dame Ouest, Montreal, QC, H3C 1K3, Canada.
[2] Gotland University, Wind Energy Technology, Cramergatan 3, 62167 Visby, Sweden.

E-mail: hugo.olivares-espinosa.1@ens.etsmtl.ca

Abstract.
An Actuator Disk (AD) model is implemented in the CFD platform OpenFOAM® with the purpose of studying the characteristics of the turbulent flow in the wake of the rotor of a horizontal-axis wind turbine. This AD model is based on the blade-element theory and it employs airfoil data to calculate the distribution of forces over the disk of a conceptual 5 MW offshore wind turbine. A uniform, non-turbulent flow is used as inflow so the turbulence is only produced in the wake of the AD. Computations are performed using Large-Eddy Simulations (LES) to capture the unsteady fluctuations in the flow. Additionally, a classic Smagorinsky Sub-Grid Scale (SGS) technique is employed to model the unfiltered motions. This new AD implementation makes use of a control system to adjust the rotational velocity of the rotor (below rated power) to the local conditions of the wind flow. The preliminary results show that the wake characteristics are influenced by the force distribution on the disk when compared to the wake produced by a uniformly loaded AD. Also, we observe that the simulated rotor reacts correctly to the introduction of the control system, although operating below the optimal power.

1. Introduction

Due to reduced availability of ideal sites (flat and obstacle free) as well as to economic profitability, wind turbines can be located close to each other in wind farms. This causes interference problems which reduce the efficiency of the array. In particular, the wind turbine wakes increase the level of turbulence and cause a momentum defect that may lead to an increase of the mechanical loads and to a reduction of the power output [1]. Therefore, it becomes important to characterize the turbulence field produced by the turbines when interacting with the Atmospheric Boundary Layer (ABL) or other turbines. The first part of the characterization process is an adequate modelling of the turbine. One of the most recurred techniques to model the rotor is the Actuator Disk (AD) in which the rotor is represented as a permeable surface where a distribution of forces acts upon the flow. In its simplest formulation, the AD comprises a surface of uniform loading modelled by one-dimensional forces in the streamwise direction. This has been proved computationally affordable and sufficient to reproduce the turbulence characteristics of the far wake [2]. Conversely, it has also been observed that the inclusion of non-uniform loading and rotation leads to a considerable improvement in the

prediction of the mean velocity and turbulence intensity in the near wake [3], [4]. On the other hand, a detailed characterization of the turbulence requires a model capable of resolving the turbulence fluctuations, so Large-Eddy Simulations (LES) are employed. Similar studies have been performed with the Actuator Line (AL) model that permits a greater detail in the reproduction of the aerodynamic features of the rotor, overcoming the problem of the lack of tip vorticity reproduction of the AD [5],[6], [8]. Despite of these advantages, the AL (as well as the actuator surface) is still too computationally expensive to be used in the simulation of wind farms. Furthermore, turbulence features in the far wake are less affected by the precision of the aerodynamics of the rotor [9]. In consequence, the characterization of individual wakes employing AD is a subject of ongoing interest in the wind energy community. The present study introduces preliminary results of an implementation of the AD in OpenFOAM® where loading and torque are calculated using the blade-element theory [10] with a control system modelled after the one presented by Breton et al. [11] to regulate the rotational velocity. These results are compared to those obtained using a uniformly loaded AD.

2. Model description

2.1. Flow model

In the Large-Eddy Simulations (LES), the large eddies (the energy-containing motions) are resolved, whereas the effects of the smaller eddies are modelled. This is performed by decomposing the Navier-Stokes equations into a filtered (or resolved) component ($\overline{u_i}(x,t)$) and a residual (or sub-grid scale, SGS) component. The resulting LES momentum equation is written as (see [12]):

$$\frac{\partial \overline{u_j}}{\partial t} + \frac{\partial \overline{u_i}\,\overline{u_j}}{\partial x_j} = -\frac{1}{\rho}\frac{\partial \overline{p_m}}{\partial x_j} + \nu\frac{\partial^2 \overline{u_j}}{\partial x_i \partial x_j} - \frac{\partial \tau_{ij}^r}{\partial x_i}, \tag{1}$$

where τ_{ij}^r is the anisotropic residual stress tensor and is given by $\tau_{ij}^r \equiv \tau_{ij}^R - \frac{2}{3}k_r\delta_{ij}$. τ_{ij}^R is the residual stress tensor $\tau_{ij}^R \equiv \overline{u_i u_j} - \overline{u_i}\,\overline{u_j}$, where k_r is the residual kinetic energy and $\overline{p_m}$ is the modified pressure. The filtered continuity equation is $\frac{\partial \overline{u_i}}{\partial x_i} = 0$. In this work, the effect of the residual scales is parametrized following the classic Smagorinsky model [13]. In this manner, the SGS stress tensor is related to the filtered rate-of-strain tensor $\overline{S_{ij}} = \frac{1}{2}\left(\frac{\partial \overline{u_i}}{\partial x_j} + \frac{\partial \overline{u_j}}{\partial x_i}\right)$ by means of $\tau_{ij}^r = -2\nu_{sgs}\overline{S_{ij}}$, where the subgrid viscosity is calculated as $\nu_{sgs} = \ell_s^2(\overline{S_{ij}}\,\overline{S_{ij}})^{1/2} = (C_S\Delta)^2\,(\overline{S_{ij}}\,\overline{S_{ij}})^{1/2}$. In this way, the *Smagorinsky length-scale* ℓ_S is assumed to be proportional to the *Smagorinsky coefficient* C_S and to the filter width Δ which is obtained from the local cell length $\Delta = (\Delta_x\Delta_y\Delta_z)^{1/3}$. The value of C_S is set to 0.168. Following this notation, time averages will be indicated with brackets, $\langle u_i \rangle$, whereas fluctuating velocities will be written with primes, u_i' .

2.2. Actuator disk

The rotor of a horizontal-axis wind turbine is modeled as an Actuator Disk (AD), where the effect of the blades in the wind flow is reproduced by forces distributed over a disk. The AD model does not consider the location of the blades at a given time to calculate these forces. Instead, the load of the turbine is taken as a time averaged quantity in the azimuthal direction.

Two different AD concepts are implemented in the course of our work with the goal of performing comparisons of the turbulence characteristics in their wakes. In the first case, it is assumed that the forces over the AD are only in the axial direction and are distributed uniformly over the disk. If U_0 is the uniform inflow velocity, the force is calculated as:

$$F_x = \frac{1}{2}\rho U_0^2 A C_T \tag{2}$$

where A is the area of the disk and C_T is the thrust coefficient (for C_T calculation, see section 3). In the second approach, the forces are calculated following the blade-element theory [10], where the lift and drag are obtained from tabulated airfoil data. In this formulation, the forces per unit area acting on the AD are calculated from

$$d\mathbf{F} = \frac{1}{2}\rho u_{rel}^2 \frac{Bc}{2\pi r}(C_L\mathbf{e_l} + C_D\mathbf{e_d})dA \tag{3}$$

where B is the number of blades and C_L, C_D are the lift and drag coefficients that are evaluated in function of the angle of attack, with $\mathbf{e_l}$ and $\mathbf{e_d}$ being the unit vectors pointing in the directions of lift and drag, respectively. The factor $\frac{B}{2\pi r}$ is commonly derived from spatially integrating over an annular element of area $dA = 2\pi r dr$ [10]. It is convenient to observe that some authors have also derived the above expression by considering the average load during the time it takes the blades to cover the path within an area element. In effect, as it was shown in [14] and [15], considering the time the blades spent over any given control volume, the average force on the rotor is exactly equal to eq. (3). An interesting result of this formulation is that the force can be calculated with this expression independently from the shape of the cells in the grid. As a result, the grid can be formed by squared cells which is highly desired in order to maintain a uniform grid-filter size in LES. This formulation is especially relevant as, on the other hand, similar works make use of intermediate steps where a polar mesh is defined only to calculate the force distribution on the AD before projecting it back to the squared mesh [8], [16].

In the case of the AL, Troldborg [6] has observed that the use of a polar mesh does not largely affect the flow solution. Unlike the aforementioned AD implementations, the conception used here does not consider a special treatment for the cells at the edge of the AD or a distribution of forces in the axisymmetric direction (commonly performed using the convolution of eq. (2) with a Gaussian expression). A model that includes an approach for these two issues will be included in a later stage. It is important to note that it is expected that the inclusion of a force distribution scheme will have an impact on the flow solution only in the vicinity of the AD.

This AD implementation also includes the use of a control system for the rotational velocity with respect to the local conditions, henceforth called *controller*. This method aims at simulating how the turbine would react in a real operation below rated power, this is, for velocities under 11.4 m/s (with a cut-in velocity is 3 m/s). Although not strictly necessary in the present case, where a uniform inflow is used, the controller is implemented here as one of the first steps in the development of a more versatile model. Indeed, as it is expected that future work will involve the use of turbulent inflows, this type of control mechanism will be a requirement. The implementation of the controller used here follows the one used in [11] and it makes use of the total aerodynamic torque T_{aero} calculated from eq. (3) for a given windspeed and rotational velocity Ω as well as its comparison to the torque produced by the turbine generator T_{gen}. In this way, if T_{aero} is different from T_{gen} at a given time, an acceleration $\Delta\Omega$ in the rotor will result according to

$$T_{aero} - T_{gen} \approx (I_{rotor} + I_{gen})\frac{\Delta\Omega}{\Delta t}, \tag{4}$$

where I_{rotor} and I_{gen} are the inertia of the rotor and generator, respectively, and Δt is the time-step. For incoming velocities above rated power, a controller that uses a pitch control system should be considered. Such a system will be incorporated in the future. It should be noted that the data of torque vs. generator speed used in this work is taken directly from [17], where the figures were calculated using a blade-element momentum method. As these values are calculated with a different scheme than the flow solver used in this work, some differences might arise regarding the torque produced for the given inflow velocity and tip-speed-ratio. In effect, analogously to what is done in [11], this curve should be calculated using the flow solver and the AD implementation used in our computations to improve the accuracy of the results. These calculations will be carried out in subsequent work.

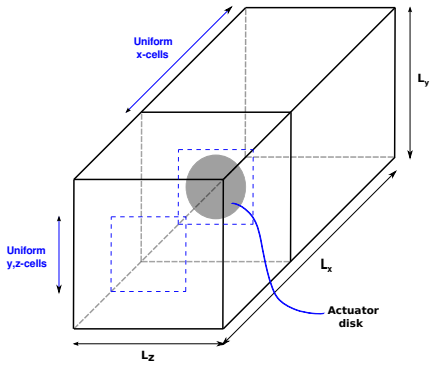

Figure 1. Scheme of the computational domain

2.3. The reference turbine model
Airfoil parameters are obtained from the concept of a 5 MW offshore wind turbine designed by the National Renewable Energy Laboratory (NREL) [17]. This is a conventional horizontal-axis, three bladed (twisted and tapered), pitch-controlled and variable speed turbine created from design information of other turbines, mainly the REpower 5M. The radius of the rotor is 63 m with a maximum power coefficient of $C_P = 0.482$, found when the tip-speed-ratio has a value of $\lambda = 7.55$ and the blade pitch angle is zero. Information regarding the torque vs. generator speed response of the turbine for a fixed inflow velocity of 8 m/s is also contained in that report. These data are then used to regulate the angular velocity of the turbine according to eq. 4, as previously indicated.

3. Numerical Setup
The computational domain consists of a rectangular mesh of size $L_x \times L_y \times L_z = 30.4 \times 17 \times 17$ R that corresponds to the streamwise, vertical and spanwise directions. A central region where cells are equally spaced in the flow direction x starts at 6.4 R from the inlet and continues until the outlet. The region is separated from all the lateral boundaries by a distance of 6.9 R. Outside this region, the cells stretch towards the boundaries with an aspect ratio of $\Delta x_{max}/\Delta x_{min} = 9.328$ and $\Delta y_{max}/\Delta y_{min} = 10.339$. The total number of cells in each direction is $N_x \times N_y \times N_z = 256 \times 64 \times 64$. The AD is located at 8 R from the inlet, in the center of the $y-z$ plane, so the wake develops within the region of uniform cells. According to the resolution of this region, the volume of the disk is approximated by a set of 316 cells. A grid with the same characteristics has been used for the studies of Breton et al. [11]. A uniform inflow at $U_0 = 8$ m/s is set at the inlet. The lateral boundaries are set to periodic while the outlet employs a convective flow condition, e.g. $\frac{\partial \phi}{\partial t} + \overline{u}_n \frac{\partial \phi}{\partial n} = 0$ ($\overline{u}_n$ is component of the instantaneous velocity normal to the outlet) for any variable ϕ in the normal direction to the boundary. The simulation of the AD with rotation has an initial value of $\Omega = 10$ RPM. The average thrust found with these calculations is later used as the fixed value imposed in the case of the uniform thrust AD, which corresponds to $C_T = 0.61$. Simulations are carried out using OpenFOAM 2.1.0, a second-order finite-volume open-source CFD code. The Quadratic Upstream Interpolation for Convective Kinematics (QUICK) scheme is used for the convective terms, which in OpenFOAM is third-order accurate when the mesh is uniform. Simulations are run with a Courant-Friedrichs-Lewy (CFL) number of 0.25 and are let run during 40 flow times (L_x/U_0) to let the turbulence to develop before the sampling of data. Measurements are taken during 20 longitudinal flow times.

4. Preliminary results and discussion
The use of LES coupled with the classic Smagorinsky SGS model in OpenFOAM has been tested by previous authors [18], where the validity of the transfer of turbulent kinetic energy

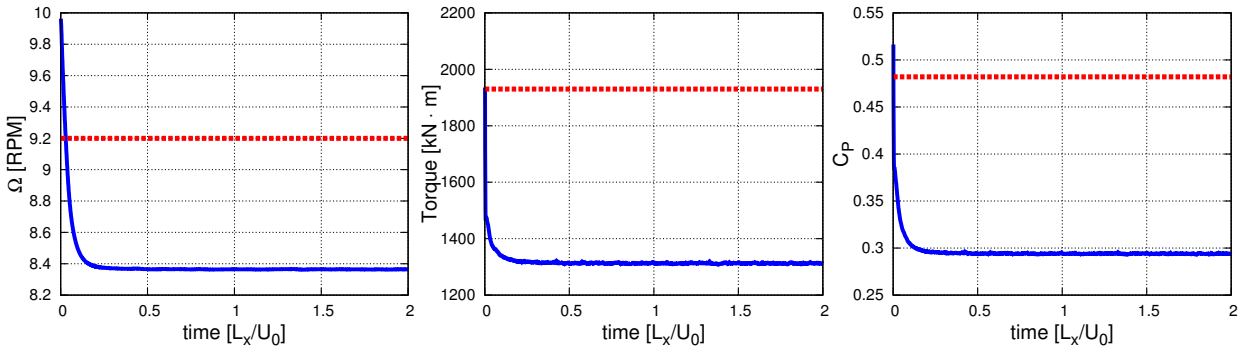

Figure 2. Rotational velocity, torque and power coefficient results for the NREL 5 MW turbine. Results are compared to those reported as being reached at the maximum power operation (straight dashed-lines). Only the first two flow times are shown as the values reached here are maintained throughout the simulation.

from the large to the small eddies has been verified by performing simulations of decaying isotropic turbulence and comparing the results with the experiments of Comte-Bellot and Corrsin [19]. Results indicate that the standard Smagorinsky-LES model in OpenFOAM is capable of simulating the turbulent-cascade by reproducing the respective Kolmogorov spectra.

The adequate size of the computational domain is verified by means of calculating the mass flow that leaves from the lateral boundaries and from the outlet with respect to the one set at the inflow. To this aim, simulations of the AD with rotation were performed on a 50% smaller and on a 50% larger computational domains with respect to the one previously described. In all the cases, it was found that the flow exiting from the sides was much less than 1% of the inlet flow. As for the number of cells, grids with a similar resolution have been found adequate for the simulation of wind turbines in the ABL flow using the same AD models in LES simulations [4]. A grid convergence study will be performed at a later stage.

The results are first compared to the rotational velocity, torque and power indicated in the technical report of the turbine modelled. In Figure 2 we can observe the evolution of these values (as a result of the adjustments derived from the controller) compared to the values exhibited during the operation at maximum power, where our turbine operates with a tip-speed-ratio of $\lambda = 6.93$, lower than expected. The causes of this discrepancy are thought to be related to: a) the values of torque vs. generator speed response used for the controller are not accurate (as discussed in section 2.2) and b) the lack of an axial force distribution around the AD, that affects the response of the controller as the local velocities are not accurately represented (due to the oscillations they exhibit at the AD location).

Figures 3 and 4 show a comparison of the development of the wake downstream of the AD. The characteristic turbulent structures appear only close to the end of the domain, at about 15 R from the disk in both cases. More complete actuator models have shown an earlier breaking of the wake into turbulent structures, which is only natural as the AD cannot reproduce the tip vortices that have been seen to contribute to trigger instabilities in the wake [6]. It is also observed in [6] that finer meshes allow tip vortices to break closer to the rotor. Moreover, it is argued also that QUICK differencing schemes suffer from numerical diffusion (artificial viscosity) that could prompt the loss of details on the turbulent structures [7]. Alternatives that offer advantages with respect to the QUICK and central difference schemes in OpenFOAM are currently considered. A combination of both schemes has been used successfully in similar works [8] .

Figure 5 shows the comparison of the time-averaged velocity profiles at different downstream distances from the disk. Clearly, the uniformly loaded AD produces smaller velocities behind the

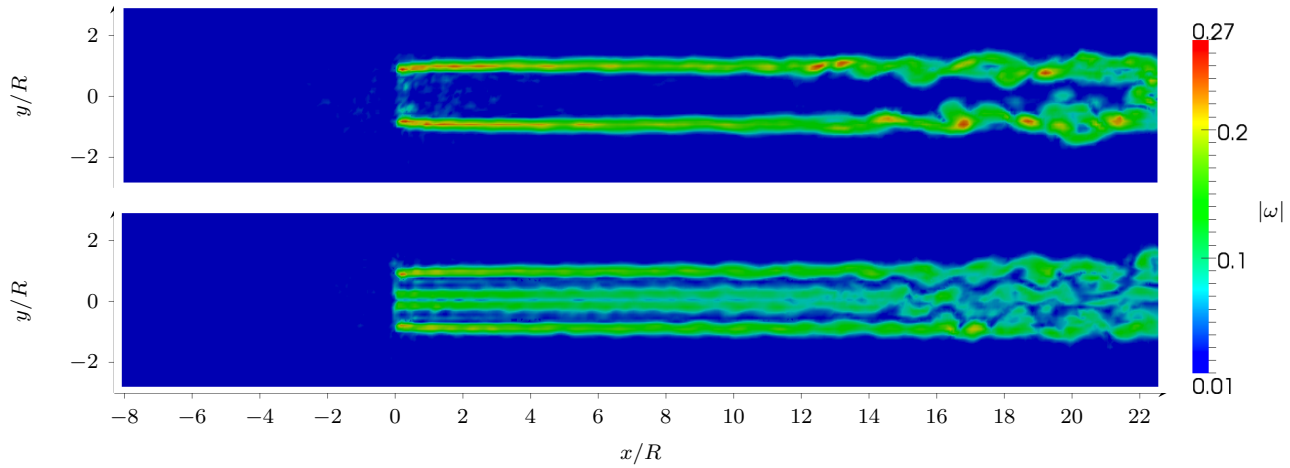

Figure 3. Contours of instantaneous vorticity magnitude of the wake development with the uniformly loaded AD (top) and the AD with rotation (bottom) at 20 L_x/U_0. Images at $L_z = 0$.

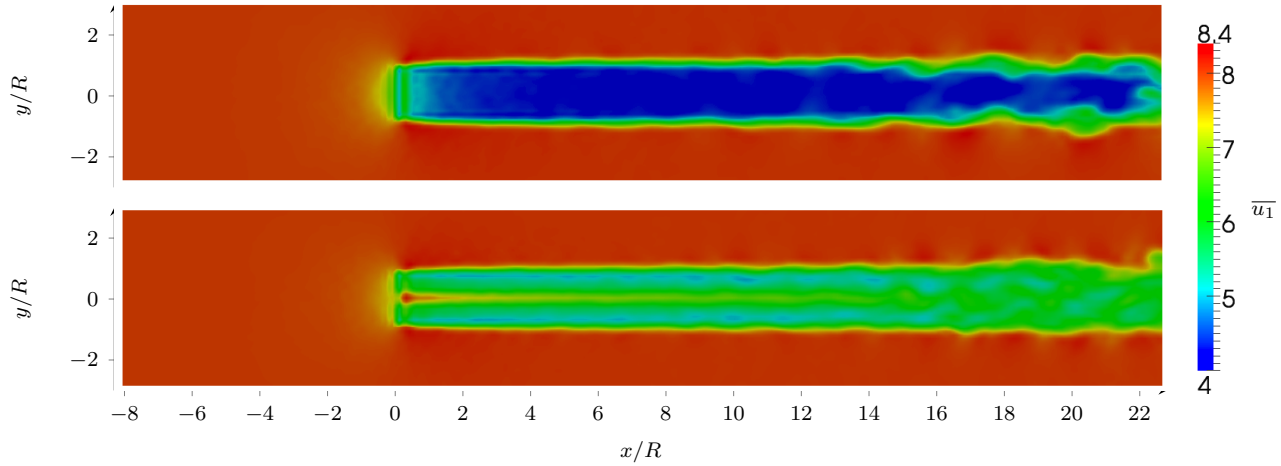

Figure 4. Comparison of the instantaneous, streamwise velocity field for the uniformly loaded AD (top) and the AD with rotation (bottom) at 20 L_x/U_0. Images are take at $L_z = 0$

rotor than the rotating AD. Moreover, the velocity profiles obtained from the AD with rotation show an acceleration of the flow in the central part of the wake. This occurs since the airfoil data provided for the turbine modelled covers also the central part of the rotor, so the prescribed values of lift and drag coefficients in that zone determine a weak thrust. In addition, in the same Figure it is observed that even the position of the last measurement at 20 R is not far enough from the disk to allow the convergence of the wakes produced by the two AD implementations.

Lastly, the comparison of the Reynolds stresses sampled at 3 locations of the wake for both models is shown in Figure 6. As it can be seen there, the values of the Reynolds stresses around the shear-layer (except $\left\langle \overline{u_1'}\ \overline{u_2'} \right\rangle$) are appreciably larger in the case of the uniformly loaded AD. This is in accordance to the larger velocity deficit in the wake of this rotor model compared to that in the wake of the AD with rotation, as seen in Figure 5. In addition, unlike the case of uniform load, in the AD with rotation there is a larger variation in the values of the stresses in the central region of the wake. This can be attributed to a combination of the effects of rotation and the distribution of forces presented in the rotating AD model. In general, $\langle \overline{u_i}\ \overline{u_i} \rangle$ increases its value with the distance from the AD, an indication of an increase of turbulence downstream in the wake. This observation is also supported by the increase of turbulence kinetic energy k,

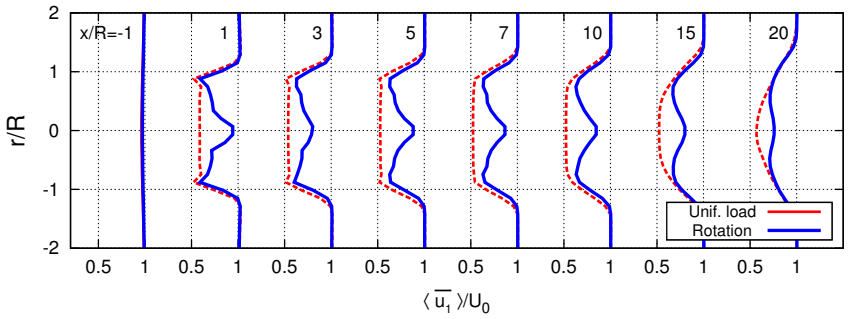

Figure 5. Vertical profiles of the time-average streamwise velocity component at $z = 0$.

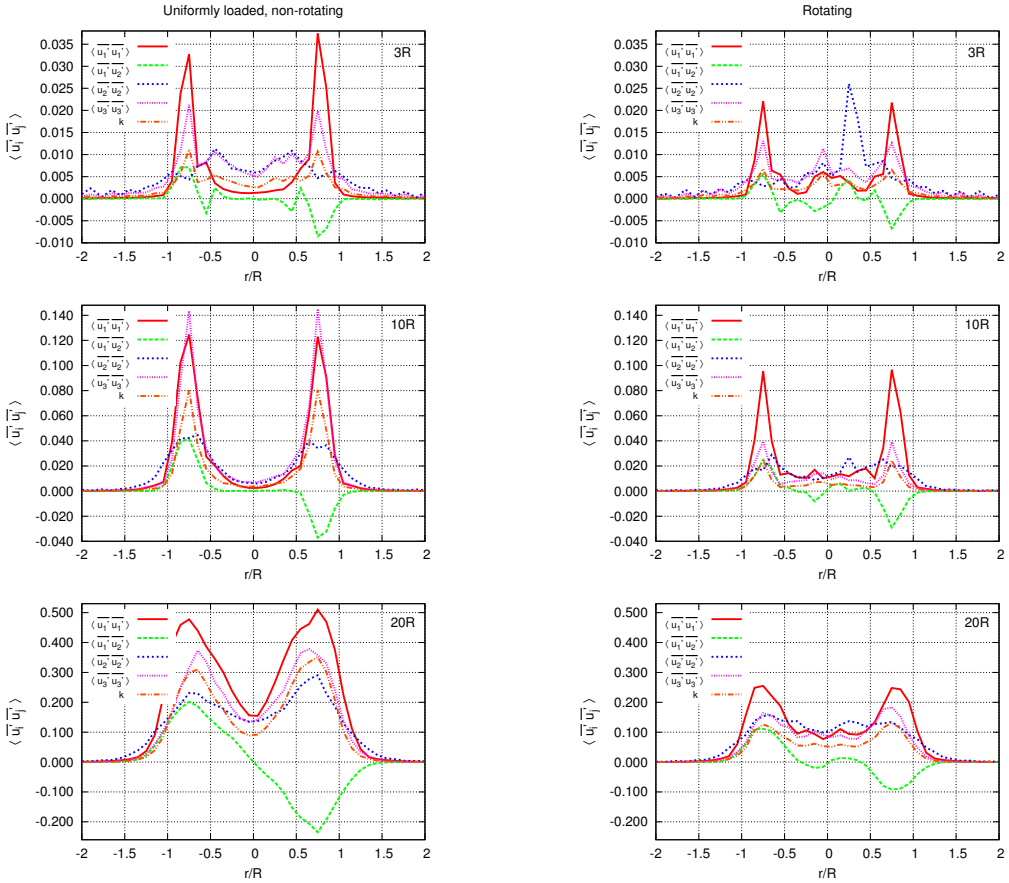

Figure 6. Reynolds stresses as a function of the vertical position, time-averaged during 20 L_x/U_0. *Left*: uniformly loaded AD. *Right*: AD with rotation. Data have been sampled at 3 R, 10 R and 20 R behind the AD (positions top to bottom). Note that the different scales are used to better appreciate the local variation of the stresses.

also shown in Figure 6. We should make note that even at 20R behind the AD, neither k nor $\langle \overline{u_i}\ \overline{u_i} \rangle$ have reached their maximum value.

5. Conclusion and future work

Two different actuator disk models have been implemented in the CFD code OpenFOAM. In the first case, an AD with a fixed thrust uniformly distributed over the surface of a disk is

modelled. In the second case, an AD where the force distribution is calculated according to the blade-element theory is simulated. Furthermore, a control system that reproduces the response of the rotational speed of the rotor to the current wind conditions is implemented following the implementation shown in [11]. A rotor was modelled after the geometric parameters and airfoil data of the NREL 5MW reference wind turbine.

The first series of results obtained from the implementation of the turbine with rotation shows that the controller indeed changes the rotational velocity of the rotor, affecting the torque and the power produced. Our results showed that the turbine operates with a lower power output than its optimum. It is possible that the lack of a force distribution scheme to smooth the velocity discontinuities affects the calculations. Other causes of these discrepancies are being investigated. A review of some features of the turbulent wake is performed. It is observed that the velocity fluctuations along the vertical profiles of the wake are larger in the case of the uniformly loaded AD.

The testing of the AD using blade-element method is in its early stages of verification, so the material presented here constitutes a preliminary set of results of an ongoing work.

6. Acknowledgements

This work is partially supported by the Consejo Nacional de Ciencia y Tecnología (CONACyT) of Mexico, the Canadian Research Chair on the Nordic Environment Aerodynamics of Wind Turbines and the Natural Sciences and Engineering Research Council (NSERC) of Canada. The authors would also like to thank the fruitful discussions with Jörn Nathan and Mary Bautista.

References

[1] Frandsen S and Thögersern M 1999 *Wind Eng.*. **23(6)** 327-340
[2] Jimenez A, Crespo A, Migoya E and Garcia J 2008 *Environ. Res. Lett.* **3** 015004
[3] Porté-Agel F, Wu Y T, Lu H and Conzemius 2011 *J. Wind Eng. Ind. Aerodyn.* **99** 154-168
[4] Wu Y T and Porté-Agel F 2011 *Boundary-Layer Meteorol.* **138** 345-366
[5] Sørensen J and Shen W 2001 *Journal of Fluid Engineering* **124** 393-399
[6] Troldborg N, Sørensen J and Mikkelsen R 2010 *Wind Energy* **13** 86-99
[7] Troldborg N 2008 Actuator Line Modeling of Wind Turbine Wakes PhD Thesis DTU Denmark
[8] Ivanell S 2009 Numerical computations of wind turbine wakes PhD Thesis KTH Sweden
[9] Vermeer L, Sørensen J and Crespo, A. 2003 *Progress in Aerospace Sciences* **39** 467-510
[10] Manwell J, McGowan J and Rogers A 2008, Wind Energy Explained, Wiley
[11] Breton S-P, Nilsson K, Ivanell S, Olivares-Espinosa H, Masson C and Dufresne L 2012 Study of the effect of the presence of downstream turbines on upstream ones and use of a controller in CFD wind turbine simulation models. Submitted to The Science of Making Torque from Wind 2012 Conference
[12] Pope S 2000 Turbulent Flows, Cambridge University Press
[13] Smagorinsky J 1963 *Mon. Weather Rev.* **91** 99–164
[14] Ammara I 1998 Mémoire de maîtrise: Modélisation aérodynamique tridimensionnelle dun parc d'éoliennes à axe horizontal (Ecole polytechnique de Montréal, Montréal, Canada)
[15] Masson C, Smaïli A and Leclerc C 2001 *Wind Eng.* **4** 1-22
[16] Réthoré P-E 2009 Wind Turbine Wake in Atmospheric Turbulence Ph.D. Thesis Risø DTU and Aalborg University Roskilde Denmark
[17] Jonkman J, Butterfield S, Musial W and Scott G 2009 Definition of a 5-MW reference wind turbine for offshore system development Tech. Rep. NREL/TP-500-38060 NREL
[18] Bautista M, Nathan J, Olivares-Espinosa H, Masson C and Dufresne L 2012 Proceedings of the 20th Annual Conf. of the CFD Soc. of Canada CFD2012
[19] Comte-Bellot G and Corrsin S 1971 *Journal of Fluid Mechanics* **48(2)** 273-337